Structure of Type I Antifreeze Protein and Mutants in Supercooled Water

Steffen P. Graether,*† Carolyn M. Slupsky,*† Peter L. Davies,†‡ and Brian D. Sykes*†
*CIHR Group in Protein Structure and Function, Department of Biochemistry, University of Alberta, Edmonton, Alberta, T6G 2H7, Canada; †Protein Engineering Network of Centres of Excellence, Inc., University of Alberta, Edmonton, Alberta, T6G 2H7, Canada; and ‡Department of Biochemistry and Department of Biology, Queen's University, Kingston, Ontario K7L 3N6, Canada

ABSTRACT Many organisms are able to survive subzero temperatures at which bodily fluids would normally be expected to freeze. These organisms have adapted to these lower temperatures by synthesizing antifreeze proteins (AFPs), capable of binding to ice, which make further growth of ice energetically unfavorable. To date, the structures of five AFPs have been determined, and they show considerable sequence and structural diversity. The type I AFP reveals a single 37-residue α-helical structure. We have studied the behavior of wild-type type I AFP and two "inactive" mutants (Ala17Leu and Thr13Ser/Thr24Ser) in normal and supercooled solutions of H_2O and deuterium oxide (D_2O) to see if the structure at temperatures below the equilibrium freezing point is different from the structure observed at above freezing temperatures. Analysis of 1D ^{1}H- and ^{13}C-NMR spectra illustrate that all three proteins remain folded as the temperature is lowered and even seem to become more α-helical as evidenced by $^{13}C_\alpha$-NMR chemical shift changes. Furthermore, ^{13}C-T_2 NMR relaxation measurements demonstrate that the rotational correlation times of all three proteins behave in a predictable manner under all temperatures and conditions studied. These data have important implications for the structure of the AFP bound to ice as well as the mechanisms for ice-binding and protein oligomerization.

INTRODUCTION

Several fish and insect species are freeze-intolerant yet are able to survive subzero temperatures. One protective strategy involves the production of antifreeze proteins (AFPs) in the serum, also known as thermal hysteresis proteins, which prevent the formation of macroscopic ice crystals. The inhibition of ice growth is believed to occur by the Kelvin effect (Raymond and DeVries, 1977), in which the binding of AFP to ice causes the ice between the bound proteins to grow in a curved front, which is energetically unfavorable. This mechanism is believed to apply to all AFPs (Davies and Sykes, 1997; Ewart et al., 1999; Yeh and Feeney, 1996). The Kelvin effect results in a nonequilibrium depression of the freezing point below the melting point and is known as thermal hysteresis. To measure the amount of thermal hysteresis of a particular AFP, the temperature of a solution of AFP is first manipulated until a single ice crystal is present. The sample is heated, and the temperature at which the crystal melts is taken as the melting point. Subsequently, the sample is cooled until the crystal begins to grow rapidly, and this temperature is noted as the nonequilibrium freezing point. The difference between the two temperatures is defined as the thermal hysteresis and is used as an indicator of the antifreeze activity of the protein.

Although it is generally accepted that AFPs bind to ice and that ice growth inhibition occurs because of the Kelvin effect, the actual binding mechanism is not well understood. The type I AFP of the winter flounder is considered to be the prototypical AFP and has served as a model for the interaction between this class of proteins and ice. The protein is completely α-helical, with four Thr residues spaced 11 residues apart on the same side of the helix (Fig. 1 *A*; Sicheri and Yang, 1995;Yang et al., 1988). Analysis of the structure and its ice-binding properties led to the hypothesis that the protein binds to a specific plane of ice through hydrogen bonds between the threonyl oxygens and ice (DeVries and Lin, 1977; Knight et al., 1991; Wen and Laursen, 1992; Sicheri and Yang, 1995). Further experimentation, however, has questioned the relative importance of this interaction. Mutagenesis of the threonines (Thr) to serine (Ser), which preserves the hydrogen bonding nature of the side chain, caused a large loss in activity (Chao et al., 1997; Haymet et al., 1998; Zhang and Laursen, 1998). In contrast, mutation of Thr to valine (Val), which preserves the isosteric nature of the side chain but cannot form a hydrogen bond, resulted in only a moderate loss in activity (Chao et al., 1997; Haymet et al., 1998; Zhang and Laursen, 1998). Mutation of Ala17 to Leu, a residue adjacent to the Thr-rich face, abolished all antifreeze activity (Baardsnes et al., 1999), which led the authors to suggest that the ice-binding face of type I AFP consists of Ala17, Ala21, the γ-methyl of Thr13, and equivalent residues at 11-amino-acid intervals.

Finally, it is thought that hydrogen bonds might form more favorably between both ice and water and the protein and water than between ice and AFP, because water molecules are able to align optimally to form a "perfect" bond, whereas a protein may not (Sonnichsen et al., 1996). Therefore, at best, the $\Delta\Delta G°$ of the interaction between the AFP and ice will be equal to $\Delta\Delta G°$ of the interaction between the AFP and water. It is unclear what would drive the binding of this protein to ice.

Received for publication 21 March 2001 and in final form 16 May 2001.
Address reprint requests to Dr. Brian D. Sykes, CIHR Group in Protein Structure and Function, Department of Biochemistry, University of Alberta, Edmonton, Alberta, Canada T6G 2H7. Tel.: 780-492-6540; Fax: 780-492-1473; E-mail: brian.sykes@ualberta.ca.

0006-3495/01/09/1677/07 $2.00

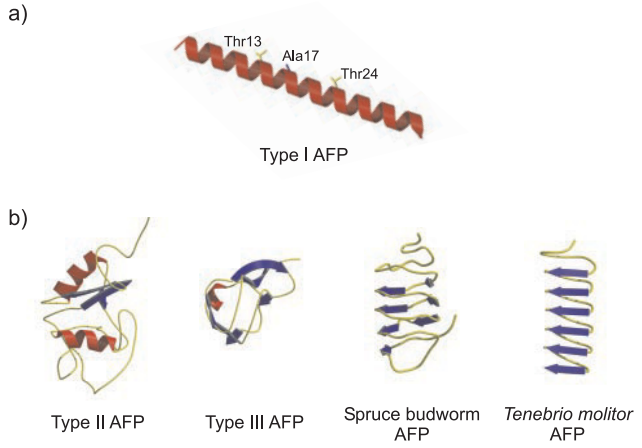

FIGURE 1 (*A*) Winter flounder type I AFP structure. The wild-type protein is shown, with the location of the mutated residues shown in a *blue* (Ala17) or *yellow* (Thr13/Thr24) stick representation. (*B*) The known structures of several AFPs.

The structures of AFPs can vary between organisms and do not necessarily include regularly spaced Thrs as in the type I AFP (Fig. 1 *B*). The type II fish AFP of the sea raven has been shown to have the fold of the Ca^{2+}-dependent lectin family (Gronwald et al., 1998), whereas the eel pout type III AFP structure has a unique fold consisting of small β-sheets (Sonnichsen et al., 1996; Jia et al., 1996). Neither have an intuitively repetitive arrangement of side chains that could match the spacing of an ice lattice. The recently determined insect AFPs from the spruce budworm (Graether et al., 2000) and *Tenebrio molitor* (Liou et al., 2000) both have a β-helical fold and, similar to the type I AFP, these proteins have a regular repetition of Thr residues. With the insect AFPs, there are two ranks of Thr, which may allow the protein to bind to two different planes of ice (Graether et al., 2000).

Given that hydrogen bonding seems to be insufficient to explain the type I AFP mutant data and the existence of diverse structures of AFPs, recent models suggest that the planarity of the ice-binding surface may be important for the binding of the protein to ice. One explanation for the effects of these mutations involves a change in the shape complementarity between type I AFP and ice. The Val mutants, with side chains isosteric to Thr, cause less change to the ice-binding surface then mutations to Ser, which would cause parts of the surface to become recessed. These results, however, do not explain the affinity of the protein for ice and suggest that other forces such as van der Waals interactions may have a role. It is possible that the binding requires both types of interactions. Based on an extensive mutational analysis of the type III AFP (Graether et al., 1999; DeLuca et al., 1998), a two-step model was proposed whereby hydrogen bonds are able to find a specific plane of ice, after which van der Waals contacts hold the protein bound to ice.

Before a more detailed model of the AFP/ice interaction can be proposed, the behavior of type I AFP at low temperatures and when it is bound to ice need to be studied. We have examined ^{1}H- and ^{13}C-nuclear magnetic resonance (NMR) spectra of wild-type type I AFP and the mutants Ala17Leu and Thr13Ser/Thr24Ser in supercooled H_2O and D_2O. In addition, we have collected NMR relaxation data at several magnetic field strengths, measuring the rotational correlation times of these proteins, to determine whether the proteins follow the Stokes-Einstein law in supercooled solutions (Skalicky et al., 2000). The results suggest that the structures of the wild-type and the mutant proteins in solution are maintained at temperatures within the thermal hysteresis gap where the protein could bind to ice, and that the rotational correlation times do not deviate from Stokes-Einstein behavior.

MATERIALS AND METHODS

Peptide synthesis

The wild-type winter flounder AFP HPLC-6, mutants Ala17Leu (Baardsnes et al., 1999), and Thr13Ser/Thr24Ser (Chao et al., 1997) were synthesized according to standard solid-phase peptide synthesis methods as described previously (Hodges et al., 1988; Gronwald et al., 1996). For ^{13}C-labeled samples, a $^{13}C_\alpha$-alanine residue (Cambridge Isotopes Laboratories, Andover, MA) was incorporated at position 17 (wild-type protein) or position 21 (mutant). The locations of the mutations are shown in Fig. 1 *A*.

NMR spectroscopy

For the NMR experiments, solutions of 1.5 mM wild-type type I AFP or the mutants Ala17Leu or Thr13Ser/Thr24Ser were made in 90% H_2O/10% D_2O (v/v) or 100% D_2O. The final pH of the samples was between 6.0 and 6.3. The pH measurements were not corrected for the effects of D_2O. 2,2-dimethyl-2-silapentane-5-sulfonic acid was added for internal referencing (0.1 mM for 90% H_2O/10% D_2O samples, 1.0 mM for 100% D_2O samples) and NaN_3 (2 mM) was used as a bacterial growth inhibitor. No additional salt was added. Medium-walled tubes (524-PP-8, Wilmad, Buena, NJ) were used to prevent tube breakage during freezing.

The ^{1}H 1D-, ^{13}C 1D- and ^{13}C-T_2 NMR spectra were collected on a Unity spectrometer (Varian, Inc., Palo Alto, CA) operating at 300 MHz using an indirect detection probe for the samples in 100% D_2O. ^{13}C-T_2 NMR spectra for the samples in 90% H_2O/10% D_2O were also collected on a Varian Unity-plus and Inova spectrometers operating at 600 MHz and 800 MHz, using a triple resonance *z* axis gradient probe and a *xyz* axes gradient probe, respectively.

For the ^{1}H and ^{13}C 1D-NMR experiments, data were collected over a temperature range of 25°C to −3°C in decrements as indicated in the respective figures. After each temperature change, samples were allowed to equilibrate for 20 min. For the ^{1}H-NMR spectra, 16,000 complex data points were acquired with 256 transients using a sweep width of 4000 Hz. The 90° pulse width was calibrated to 7.8 μs. Continuous wave ^{1}H decoupling for water suppression was applied at γB_1 = 100 Hz during the 2.5 s presaturation delay. For the ^{13}C-NMR spectra, a sweep width of 16,000 Hz was used and the acquired data consisted of 8000 complex data points and 13,312 transients. The pulse sequence recycling delay was 550 ms. After a 50-ms delay at the beginning of the pulse sequence, Waltz-16 ^{1}H decoupling was applied at γB_1 = 1.7 kHz for the remainder of the sequence. The 90° carbon pulse was calibrated to be 13.9 μs.

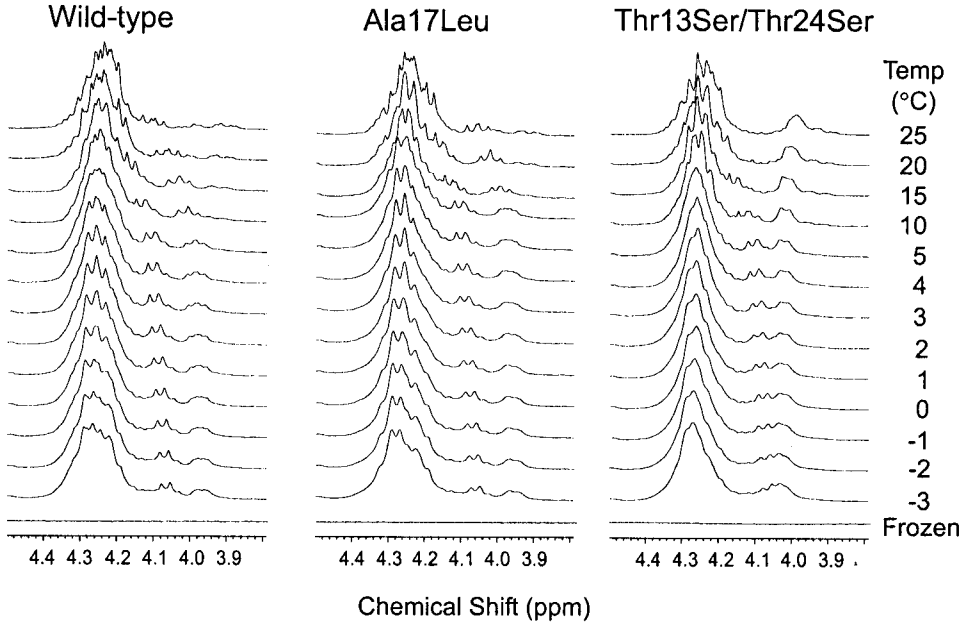

FIGURE 2 ^{1}H-NMR spectra at 300 MHz of type I AFP and mutants Ala17Leu and Thr13Ser/Thr24Ser in 100% D_2O. Samples were cooled from 25°C to −3°C as outlined in Materials and Methods.

For the ^{13}C-T_2 NMR relaxation data, a temperature range of 20°C to −5°C was used with an equilibration period of 30 min after each temperature change. For these measurements, the ^{15}N-T_2 pulse sequence (Farrow et al., 1994) was modified in-house for the measurement of ^{13}C-T_2 relaxation in CH groups. On the Unity 300 MHz spectrometer (sample in 100% D_2O), 1952 transients were collected with a sweep width of 4000 Hz and 424 complex data points at each temperature. The ^{13}C carrier was placed at 54 ppm. A calibrated ^{1}H 90° pulse width of 7.5 μs was used. The delay for the insensitive nucleus enhancement by polarization transfer (INEPT), which was constant at all temperatures used, was set to 1.79 ms. The Carr-Purcell-Meiboom-Gill (CPMG) pulse train consisted of a series of ^{13}C 180° pulses of γB_1 = 7.6 kHz every 0.9 ms and did not contain any ^{1}H pulses. Between 25°C and 10°C, the duration of the CPMG pulse train was 3.9, 11.7, 19.5, 31.2, 46.8, 62.4, 93.6 μs. Between 5°C and −5°C, the duration of the CPMG pulse train was 3.9, 11.7, 19.5, 31.2, 42.9, 54.6, 66.3 μs. No gradients or presaturation were applied. ^{13}C decoupling during acquisition was performed with Waltz-16 decoupling at γB_1 = 817 Hz.

On the Unity 600 MHz spectrometer (sample in 90% H_2O/10% D_2O), 512 transients were collected with a sweep width of 7500 Hz and 960 complex data points at each temperature. The 90° ^{1}H pulse width was calibrated for each temperature according to the formula:

$$\text{pulse width } (\mu s) = -0.195\,(T - 273) + 12.8$$

The ^{13}C carrier was placed at 58 ppm. The delay for the INEPT transfer, which was constant at all temperatures used, was set to 1.79 ms. The CPMG pulse train consisted of a series of ^{13}C 180° pulses of γB_1 = 3.88 kHz every 0.9 ms and did not contain any ^{1}H pulses. The duration of the CPMG pulse train was 4.1, 12.3, 20.5, 32.8, 41.0, 49.2, and 57.4 μs. Presaturation of H_2O at γB_1 = 35 Hz was used during the pulse sequence recycle delay of 3.0 s. ^{13}C decoupling during acquisition was performed using the globally optimized alternating-phase rectangular pulses (GARP-1) decoupling sequence at γB_1 = 2.3 kHz. The ratios of the duration of the phase encoding and decoding z axis gradients used for sensitivity enhancement were set to γ_H/γ_C = 4.0.

The ^{13}C-T_2 measurement on the 800-MHz spectrometer was made using the protein pack gChsqc pulse sequence. The pulse sequence is similar to that of Farrow et al. (1994), except that a cassette of ^{13}C 180° pulses of γB_1 = 3.42 kHz was applied every 0.5 ms with a ^{1}H 180° pulse applied every 4 ms. Sixteen transients with a sweep width of 11,000 Hz and 2048 complex data points were collected at 25°C. A proton 90° pulse width of 7.2 μs and a ^{13}C 90° pulse width of 73.1 μs were used. The ^{13}C carrier was placed at 55 ppm. The delay for the INEPT transfer was set to 1.9 ms. The duration of the CPMG pulse train was 10 to 100 μs in length in increments of 10 μs. Presaturation of H_2O was used during the pulse sequence recycle delay of 1.5 s. ^{13}C decoupling during acquisition was performed using the Waltz-16 decoupling sequence at γB_1 = 2.4 kHz.

The T_2 value was determined by fitting the data to the equation:

$$M_{xy}(t) = M_o \times e^{-t_{relax}/T_2}$$

Where $M_{xy}(t)$ is the magnetization in the x, y plane at time t, M_o is the initial x, y plane magnetization, t_{relax} is the duration of the CPMG pulse train, and T_2 is the spin-spin relaxation time.

RESULTS

Freezing profile of the wild-type type I AFP

To determine whether there was any change in structure for type I AFP present in normal versus supercooled water, we first examined the ^{1}H-NMR spectra of the wild-type protein (Fig. 2 *A*). For clarity, only the region of the spectrum from 3.8 to 4.5 ppm is shown, corresponding to the H_α resonances from all residues and the H_β resonances from Thr and Ser residues. This region was chosen because H_α resonances are particularly sensitive indicators of protein secondary structure (Wishart et al., 1991). A number of resonances overlap between 4.15 to 4.35 ppm, corresponding mainly to the H_α resonances of the 23 alanines in the sequence (Gronwald et al., 1996), suggesting that H_α is in

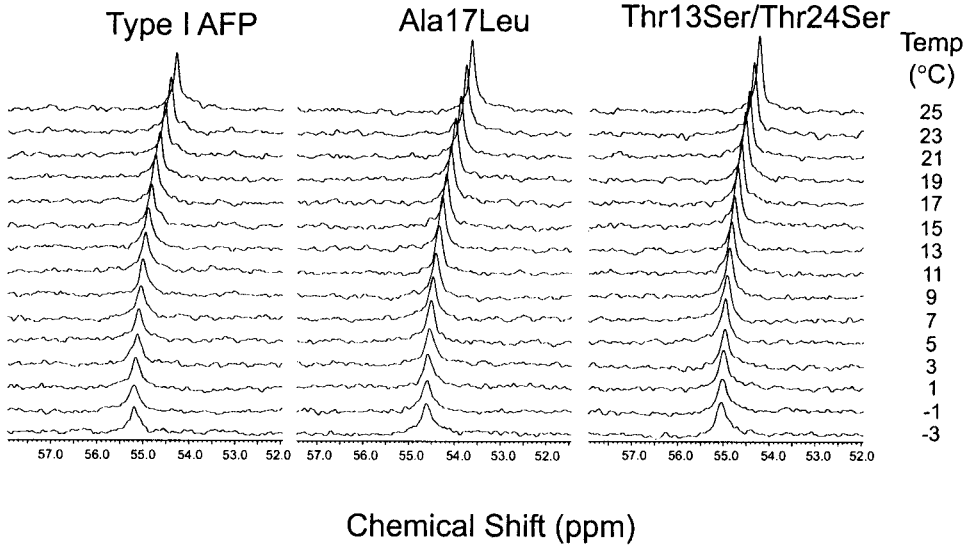

FIGURE 3 ^{13}C-NMR spectra at 300 MHz of type I AFP and mutants Ala17Leu and Thr13Ser/Thr24Ser in 100% D_2O. Samples were cooled from 25°C to −3°C as outlined in Materials and Methods.

chemical environments corresponding to largely α-helical structure. As the temperature is decreased, these resonances shift upfield, indicating that the structure is becoming more α-helical. In addition, the ^{1}H-NMR spectrum shows a broadening of the lines. As will be shown, this is a result of the increase in the viscosity of the solvent and does not represent a change in structure.

The ^{13}C-NMR spectrum of the $^{13}C_\alpha$-labeled wild-type AFP is shown as a function of temperature in Fig. 3 *A*. As with the ^{1}H-NMR spectra, the data show that there is a peak broadening but no evidence of either a loss in structure or dimerization. The chemical shift of the carbon peak moves from 54.3 to 55.2 ppm, where a value of 53.2 ppm indicates that the residue is in an α-helical conformation (Wishart et al., 1991). The data demonstrate that the protein is actually becoming more α-helical as the temperature decreases from 25°C to −3°C.

The experiments were conducted to temperatures as low as −10°C to ensure that all samples would eventually freeze, but because of the stochastic nature of freezing and the presence of heterogeneous ice-nucleators, samples would freeze anywhere from −3°C to −8°C. This is shown in Fig. 2 as the last spectrum, indicating that we were no longer able to perform liquid state NMR measurements. The fact that the solutions of both wild-type and mutant proteins did not freeze at temperatures below 0°C should not be equated with antifreeze activity. A control sample that consisted of only 0.1 M DSS in D_2O, the minimum concentration used in all experiments, could also be supercooled to at least −5°C (data not shown). Therefore, the lack of ice formation relates simply to the supercooling of the solution and does not represent thermal hysteresis attributable to the presence of an AFP, which at 1.5 mM wild-type protein would be ~0.6°C.

Relaxation measurements of wild-type type I AFP

The ^{13}C-T_2 relaxation times of the protein were measured in normal and supercooled solutions. These measurements were performed at three magnetic field strengths on $^{13}C_\alpha$-Ala17 wild-type type I AFP. Analysis of T_2 measurements of wild-type protein labeled at $^{13}C_\alpha$-Ala3 showed similar results to the $^{13}C_\alpha$-Ala17-labeled protein (data not shown), suggesting that the *N*-terminal residues behave similarly to the central residues.

The results are shown in Fig. 4, plotted as $1/T_2$ versus η/T, where $1/T_2$ is the inverse of the spin-spin relaxation time, η is the viscosity of the H_2O (Tanishita and White,

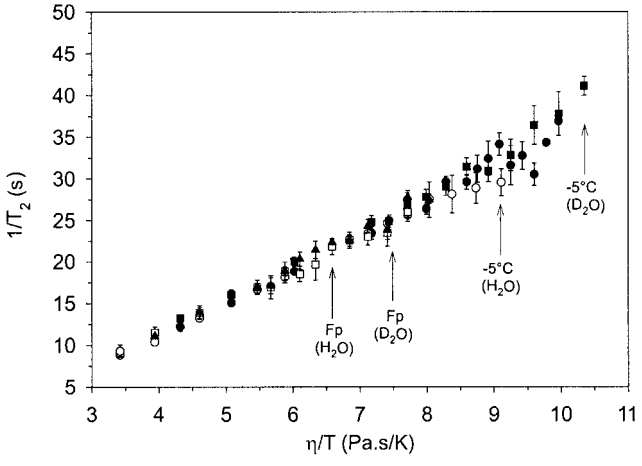

FIGURE 4 ^{13}C $1/T_2$ versus temperature, solvent, and NMR frequency. *Circles*, wild-type AFP. *Squares*, Ala17Leu. *Triangles*, Thr13Ser/Thr24Ser. *Black symbols*, 100% D_2O, 300 MHz spectrometer. *Open symbols*, 90% H_2O/10% D_2O, 600 MHz spectrometer. *Gray,* 100% D_2O, 800 MHz spectrometer. *Fp*, freezing point.

1984) or D_2O (Fernández-Prini and Dooley, 1997) solvent, and T is the temperature in Kelvin. As can be seen in the figure, the plot is linear and is independent of the magnetic field strength, whether the solvent is H_2O or D_2O, or whether the solution was at normal or supercooled temperatures. This suggests that the rotational correlation time is linearly proportional to the viscosity of the solvent. The relationship is derived from the Stokes-Einstein equation, which states:

$$\tau_c = V\left(\frac{\eta}{k_B \times T}\right)$$

where τ_c is the rotational correlation time, V is the hydrodynamic volume, η is the viscosity of the solvent, k_B is the Boltzmann constant, and T is the temperature in Kelvin. Under the nonextreme narrowing condition, $(\omega_o\tau_c)^2 \gg 1$, and assuming that hydrodynamic volume remains constant, we can simplify the relationship between the measured T_2 NMR relaxation time and solvent parameters as:

$$\frac{1}{T_2} \propto \frac{\eta}{T}$$

where $1/T_2$ is the inverse of the spin-spin relaxation time (s), η is the viscosity of the solvent Pascal · second (Pa.s), and T is the temperature (K).

Freezing profile of mutants

The freezing profiles of the ^{1}H-NMR spectra of the mutants Ala17Leu and Thr13Ser/Thr24Ser are shown in Fig. 2, *B* and *C*. Although the H_α region of the Ala17Leu mutant appears very similar to that of the wild-type protein, the Thr13Ser/Thr24Ser mutant shows an additional cluster of peaks at 4.0−4.1 ppm. These peaks are a result of the β-protons of Ser13 and Ser24 in the Thr13Ser/Thr24Ser mutant. The mutants Ala17Leu and Thr13Ser/Thr24Ser show more broadening at 25°C than the wild-type protein, suggesting that these peptides may be less structured at this temperature than the wild-type protein. At lower temperatures this difference is less significant. As with the wild-type protein, most resonances in this region shift upfield, indicating that the structure is becoming more α-helical. One exception is the cluster of peaks in the Thr13Ser/Thr24Ser mutants at 4.0−4.1 ppm, which shift downfield. Because β-proton shifts are somewhat irregular when changing from a random coil conformation to an α-helical one (Wishart et al., 1991), we can not conclude what this change represents. For the ^{13}C-NMR spectra, the freezing profiles are very similar to that of the wild-type protein in that there is a downfield shift of the labeled α-carbon as the temperature is decreased, suggesting that the structure of the mutants is becoming more α-helical. With the Ala17Leu mutant, the carbon peak moves from 54.2 ppm to 55.1 ppm from 25°C to −3°C, and as for the Thr13Ser/Thr24Ser mutant, the carbon peak moves from 54.3 ppm to 55.0 ppm over the same temperature range.

Examination of the ^{1}H- and ^{13}C data also shows that the peak areas did not change dramatically as the temperature decreased, suggesting that the amount of protein in the solution is constant. Therefore, there is no evidence of significant aggregation in solution or of the protein binding to any ice embryos in solution.

Relaxation measurements of the mutants

The ^{13}C-T_2 relaxation measurements of the mutants Ala17Leu and Thr13Ser/Thr24Ser are shown in Fig. 4 as a plot of $1/T_2$ versus η/T. As with the wild-type protein, the inverse of the spin-spin relaxation time is linearly proportional to the viscosity of the solvent. At higher temperatures, the measurements are essentially identical among all three proteins. At lower temperatures, the values show some deviation, but this is not outside the experimental error in measurement.

DISCUSSION

Several computational models have been proposed to explain how AFPs bind to ice and inhibit ice growth. Although differences exist between the models, they essentially rely on AFP binding to ice via hydrogen bonds (Wierzbicki et al., 1996; Jorgensen et al., 1993; Chou, 1992), although recent approaches are incorporating hydrophobic effects (Dalal and Sonnichsen, 2000; Madura et al., 2000). As outlined in the introduction, the roles of hydrogen bonds are in question since the substitution of the Thr with Ser in type I AFP caused a much larger loss in activity than a substitution with Val. The work presented here represents the first detailed structural study of AFPs at temperatures when it is active.

The ^{1}H-NMR spectra of the wild-type protein are shown in Fig. 2 *A*. A similar amount of broadening was observed in all regions of the spectra (data not shown). Similarly, movement of the peaks was consistent with greater structuring, rather than unfolding. A series of ^{13}C-NMR spectra were also collected of the wild-type protein. Because the proteins were only ^{13}C-labeled at the C_α atom of one residue, only one peak was observed. The spectra (Fig. 3 *A*) show that the ^{13}C resonance shifted downfield as the temperature changed from 25°C to −3°C. This agrees with the circular dichroism (CD) data, which showed that the protein becomes more α-helical as the temperature is decreased (Gronwald et al., 1996). These data also show that the change continues even when the protein is in a supercooled solution. Because this previous CD study has shown that the type I AFP is 100% helical at 3°C, the NMR data would suggest that the protein is "greater than" 100% helical at lower temperatures. However, it is more likely that this

result is a reflection of the uncertainty of the value of 100% helix at $[\theta]_{220}$ (Woody, 1995).

$^{13}C_\alpha$-T_2 measurements indicate that the rate of tumbling of the protein remains proportional to the viscosity of the solvent as it goes from a normal to a supercooled state (i.e., the protein obeys the Stokes-Einstein equation). As shown in Fig. 4, this is true irrespective of the presence of a mutation, nature of the aqueous solvent, or the temperature of the solution. In addition, this would suggest that the AFP does not alter the water shell surrounding the protein at supercooled temperatures, and that the viscosity experienced by the protein is equal to the viscosity of the solvent. Thus, the broadening of the lines in these two sets of experiments is not unexpected as the viscosity of the solvent increases as the temperature is decreased. Therefore, the structure of the type I AFP does not unfold in a supercooled solution nor does it oligomerize.

Previous studies on the viscosity of an antifreeze glycoprotein (AFGP) in solution suggested that the viscosity increased at a rate faster than what would normally be expected by the Stokes-Einstein equation as the temperature was decreased. The authors argue that part of the activity of biological antifreezes may come from the change in viscosity because an increase in viscosity decreases the rate of ice nucleation (Eto and Rubinsky, 1993). Such a viscosity change is not reflected in the measurements on type I AFP. It is possible that this change in the presence of AFGP represents an effect of the carbohydrate moiety of the glycoprotein.

Although several of the x-ray structures have been solved at subzero temperatures, they do not necessarily represent the structure bound to ice, because the protein crystals are often snap-frozen under a stream of nitrogen gas. One recent x-ray crystallographic study of the type III AFP slowly cooled the crystal from room temperature to 260 or 240 K (Antson et al., 2001). An examination of the Fourier difference maps between the diffraction data at room temperature and below freezing did not reveal any significant differences. This led the authors to suggest that there were no large-scale changes in water or protein structure, which agrees with our data.

The mutants Ala17Leu and Thr13Ser/Thr24Ser exhibited similar behavior in the ^{1}H- and ^{13}C-NMR experiments to wild-type type I AFP. That is, they showed a broadening of the lines in the ^{1}H-NMR spectra, a downfield shift of the $^{13}C_\alpha$-Ala peak and a linear relationship between $1/T_2$ and η/T. The spectral differences that were observed between the wild-type protein and the mutant Thr13Ser/Thr24Ser can be attributed to the different amino acid compositions rather than to a change in structure. In Thr13Ser/Thr24Ser, an additional cluster of peaks is seen at 4.0–4.1 ppm, corresponding to the appearance of H_β peaks from the Ser13 and Ser24 residues. With the mutants, it can be seen that at 25°C in the ^{1}H-NMR spectra there is less structure than in the wild-type protein, but this difference disappears at the lower temperatures, suggesting that the difference in structure does not correlate with the loss of antifreeze activity.

These mutations were chosen because they are proposed to inactivate type I AFP. It is thought that the Ala17Leu mutant disrupts the flatness of the type I AFP ice-binding surface (Fig. 1 *A*), and may sterically prevent the protein from binding to the ice (Baardsnes et al., 1999). The Thr13Ser/Thr24Ser mutant preserves the hydrogen bonding nature of the side chains, but may disrupt the flatness of the surface by the absence of the Thr methyl group.

The question remains as to why the mutant proteins behave similarly to the wild-type protein in these experiments, yet they are less active. One possibility is that the mutations affect the surface characteristics of the protein so that it is no longer able to bind to ice. Another possibility is that mutations subtly affect the curvature of the molecule so that it is no longer an ideal, linear α-helix. The mutation from Thr to Ser could cause the helix face to bend slightly in a concave fashion, whereas a mutation from Ala to Leu could cause the helix to bend slightly in a convex fashion. This would disrupt the arrangement of any periodic binding groups on the surface of the protein and thus the linearity of the α-helix, potentially disrupting the ice-binding surface. Such changes may not be detected by CD or the NMR experiments listed here, and would require further experimentation.

Mechanistically, it is not well understood how AFPs bind to ice. Wen and Laursen (1992) had proposed that the type I AFP packs on the ice surface to form patches of bound protein. We have shown that AFPs do not aggregate at temperatures at which the protein is active, suggesting that oligomerization is not a factor in ice-growth inhibition. We have also shown that their structure is extremely stable up until the point of freezing. The fact that the mutant AFPs are similar in the ^{1}H- and ^{13}C-NMR freezing profiles and ^{13}C-T_2 measurements implies that there must be some type of slight perturbation near the ice-binding site that reduces or eliminates antifreeze activity. It has already been shown that hydrogen-bonding via threonyl hydroxyl groups is insufficient to explain the interaction, and that van der Waals radii may better explain the effects of the mutations on the ice-binding activity.

Our experiments have been performed in supercooled water, a temperature at which the AFPs could bind to ice. However, no macroscopic ice could be present in the sample because at that point it would instantly freeze and liquid-state measurements would no longer be possible. It is also not possible to follow the freezing of the protein, because the process occurs within seconds and cannot be followed by the experimental methods used here. Our data cannot exclude the possibility of the protein changing in structure after it is bound to ice. Presently, we are looking at AFP in ice to allow us to determine the structure of the protein in the bound state.

We thank Leo Spyracopoulos for help with the pulse sequences used in the T_2 relaxation experiments. We also thank the National High Field Nuclear Magnetic Resonance Centre for the use of the 800 MHz spectrometer. This work is supported by grants from the Canadian Institutes of Health Research (CIHR), the Government of Canada's Network of Centres of Excellence program (supported by CIHR and Natural Sciences and Engineering Council through Protein Engineering Network of Centers of Excellence, Inc.) and A/F Protein Inc. to B.D.S. and P.L.D. P.L.D. is a Killam Research Fellow and S.P.G. is the recipient of a CIHR Fellowship and an Alberta Heritage Fund for Medical Research Fellowship.

REFERENCES

Antson, A. A., D. J. Smith, D. I. Roper, S. Lewis, L. S. Caves, C. S. Verma, S. L. Buckley, P. J. Lillford, and R. E. Hubbard. 2001. Understanding the mechanism of ice binding by type III antifreeze proteins. *J. Mol. Biol.* 305:875–889.

Baardsnes, J., L. H. Kondejewski, R. S. Hodges, H. Chao, C. Kay, and P. L. Davies. 1999. New ice-binding face for type I antifreeze protein. *FEBS Lett.* 463:87–91.

Chao, H., M. E. Houston, R. S. Hodges, C. M. Kay, B. D. Sykes, M. C. Loewen, P. L. Davies, and F. D. Sonnichsen. 1997. A diminished role for hydrogen bonds in antifreeze protein binding to ice. *Biochemistry.* 36:14652–14660.

Chou, K. C. 1992. Energy-optimized structure of antifreeze protein and its binding mechanism. *J. Mol. Biol.* 223:509–517.

Dalal, P., and F. D. Sonnichsen. 2000. Source of the ice-binding specificity of antifreeze protein type I. *J. Chem. Inf. Comput. Sci.* 40:1276–1284.

Davies, P. L., and B. D. Sykes. 1997. Antifreeze proteins. *Curr. Opin. Struct. Biol.* 7:828–834.

DeLuca, C. I., P. L. Davies, Q. Ye, and Z. Jia. 1998. The effects of steric mutations on the structure of type III antifreeze protein and its interaction with ice. *J. Mol. Biol.* 275:515–525.

DeVries, A. L., and Y. Lin. 1977. Structure of a peptide antifreeze and mechanism of adsorption to ice. *Biochim. Biophys. Acta.* 495:388–392.

Eto, T. K., and B. Rubinsky. 1993. Antifreeze glycoproteins increase solution viscosity. *Biochem. Biophys. Res. Commun.* 197:927–931.

Ewart, K. V., Q. Lin, and C. L. Hew. 1999. Structure, function and evolution of antifreeze proteins. *Cell Mol. Life Sci.* 55:271–283.

Farrow, N. A., R. Muhandiram, A. U. Singer, S. M. Pascal, C. M. Kay, G. Gish, S. E. Shoelson, T. Pawson, J. D. Forman-Kay, and L. E. Kay. 1994. Backbone dynamics of a free and phosphopeptide-complexed Src homology 2 domain studied by 15N NMR relaxation. *Biochemistry.* 33:5984–6003.

Fernández-Prini, R., and Dooley, R. B. 1997. Revised Release on the IAPS formulation 1985 for the viscosity of ordinary water substance. The International Association for the Properties of Water and Steam. Erlangen, Germany. 1–15.

Graether, S. P., C. I. DeLuca, J. Baardsnes, G. A. Hill, P. L. Davies, and Z. Jia. 1999. Quantitative and qualitative analysis of type III antifreeze protein structure and function. *J. Biol. Chem.* 274:11842–11847.

Graether, S. P., M. J. Kuiper, S. M. Gagne, V. K. Walker, Z. Jia, B. D. Sykes, and P. L. Davies. 2000. β-Helix structure and ice-binding properties of a hyperactive antifreeze protein from an insect. *Nature.* 406: 325–328.

Gronwald, W., H. Chao, D. V. Reddy, P. L. Davies, B. D. Sykes, and F. D. Sonnichsen. 1996. NMR characterization of side chain flexibility and backbone structure in the type I antifreeze protein at near freezing temperatures. *Biochemistry.* 35:16698–16704.

Gronwald, W., M. C. Loewen, B. Lix, A. J. Daugulis, F. D., Sonnichsen, P. L. Davies, and B. D. Sykes. 1998. The solution structure of type II antifreeze protein reveals a new member of the lectin family. *Biochemistry.* 37:4712–4721.

Haymet, A. D., L. G. Ward, M. M. Harding, and C. A. Knight. 1998. Valine substituted winter flounder "antifreeze": preservation of ice growth hysteresis. *FEBS Lett.* 430:301–306.

Hodges, R. S., P. D. Semchuk, A. K. Taneja, C. M. Kay, J. M. Parker, and C. T. Mant. 1988. Protein design using model synthetic peptides. *J. Pept. Res.* 1:19–30.

Jia, Z., C. I. DeLuca, H. Chao, and P. L. Davies. 1996. Structural basis for the binding of a globular antifreeze protein to ice. *Nature.* 384:285–288.

Jorgensen, H., M. Mori, H. Matsui, M. Kanaoka, H. Yanagi, Y. Yabusaki, and Y. Kikuzono. 1993. Molecular dynamics simulation of winter flounder antifreeze protein variants in solution: correlation between side chain spacing and ice lattice. *Protein Eng.* 6:19–27.

Knight, C. A., C. C. Cheng, and A. L. DeVries. 1991. Adsorption of α-helical antifreeze peptides on specific ice crystal surface planes. *Biophys. J.* 59:409–418.

Liou, Y. C., A. Tocilj, P. L. Davies, and Z. Jia. 2000. Mimicry of ice structure by surface hydroxyls and water of a β-helix antifreeze protein. *Nature.* 406:322–324.

Madura, J. D., K. Baran, and A. Wierzbicki. 2000. Molecular recognition and binding of thermal hysteresis proteins to ice. *J. Mol. Recognit.* 13:101–113.

Raymond, J. A., and A. L. DeVries. 1977. Adsorption inhibition as a mechanism of freezing resistance in polar fishes. *Proc. Natl. Acad. Sci. U.S.A.* 74:2589–2593.

Sicheri, F., and D. S. Yang. 1995. Ice-binding structure and mechanism of an antifreeze protein from winter flounder. *Nature.* 375:427–431.

Skalicky, J. J., D. K. Sukumaran, J. L. Mills, and T. Szyperski. 2000. Toward structural biology in supercooled water. *J. Am. Chem. Soc.* 122:3230–3231.

Sonnichsen, F. D., C. I. DeLuca, P. L. Davies, and B. D. Sykes. 1996. Refined solution structure of type III antifreeze protein: hydrophobic groups may be involved in the energetics of the protein-ice interaction. *Structure.* 4:1325–1337.

Tanishita, I., and White, H. J. 1984. Release on viscosity and thermal conductivity of heavy water substance. The International Association for The Properties of Steam. Washington, D.C. 1–18.

Wen, D., and R. A. Laursen. 1992. A model for binding of an antifreeze polypeptide to ice. *Biophys. J.* 63:1659–1662.

Wierzbicki, A., M. S. Taylor, C. A. Knight, J. D. Madura, J. P. Harrington, and C. S. Sikes. 1996. Analysis of shorthorn sculpin antifreeze protein stereospecific binding to (2 -1 0) faces of ice. *Biophys. J.* 71:8–18.

Wishart, D. S., B. D. Sykes, and F. M. Richards. 1991. Relationship between nuclear magnetic resonance chemical shift and protein secondary structure. *J. Mol. Biol.* 222:311–333.

Woody, R. W. 1995. Circular dichroism. *Methods Enzymol.* 246:34–71.

Yang, D. S., M. Sax, A. Chakrabartty, and C. L. Hew. 1988. Crystal structure of an antifreeze polypeptide and its mechanistic implications. *Nature.* 333:232–237.

Yeh, Y., and R. E. Feeney. 1996. Antifreeze proteins: structures and mechanisms of function. *Chem. Rev.* 96:601–617.

Zhang, W., and R. A. Laursen. 1998. Structure-function relationships in a type I antifreeze polypeptide: the role of threonine methyl and hydroxyl groups in antifreeze activity. *J. Biol. Chem.* 273:34806–34812.